Agricultural Water Management 98 (2010) 124–133

Contents lists available at ScienceDirect

Agricultural Water Management

journal homepage: www.elsevier.com/locate/agwat

Whole-tree water balance and indicators for short-term drought stress in non-bearing 'Barnea' olives

Alon Ben-Gal[a,*], Dilia Kool[b], Nurit Agam[a], Gerardo E. van Halsema[b], Uri Yermiyahu[a], Ariel Yafe[a], Eugene Presnov[a], Ran Erel[a], Ahmed Majdop[a], Isaac Zipori[c], Eran Segal[a], Simon Rüger[d], Ulrich Zimmermann[d], Yafit Cohen[e], Victor Alchanatis[e], Arnon Dag[c]

[a] Soil, Water and Environmental Sciences, Agricultural Research Organization, Gilat Research Center, Mobile post Negev 2, 85280, Israel
[b] Irrigation and Water Engineering, Wageningen University, The Netherlands
[c] Fruit Tree Sciences, Agricultural Research Organization, Gilat Research Center, Israel
[d] Lehrstuhl für Biotechnologie, Biozentrum, Universität Würzburg, Germany
[e] Agricultural Engineering, Agricultural Research Organization, Volcani Center, Israel

ARTICLE INFO

Article history:
Received 20 April 2010
Received in revised form 10 August 2010
Accepted 14 August 2010
Available online 15 September 2010

Keywords:
Lysimeter
Plant growth
Transpiration
Physiological monitoring
Water status
Olea europaea

ABSTRACT

Drainage-weighing lysimeters allowed monitoring of water balance components of non-bearing olive (*Olea europaea* cv Barnea) trees over a 3-month period including short-term events of controlled but severe water stress. The objective of the study was to evaluate a variety of soil and plant-based water status and drought stress monitoring methods on the basis of tree-scale evapotranspiration (ET). As the trees entered into and recovered from water stress, meteorological data, actual ET (ET_a), soil water content and changes in leaf turgor pressure were continuously monitored. Additionally, midday measurements of stem water potential, stomatal conductance, canopy temperature, and quantum yield of PSII photochemistry were conducted. Diurnal (dawn to dusk) measurements of all the above were made hourly on days of maximum stress. Shoot elongation rate was measured for periods of stress and recovery. Quantum yield of PSII photochemistry, stomatal conductance, and stem water potential all successfully indicated reductions in whole-tree water consumption beginning at moderate stress levels. These measured parameters fully recovered to the levels of non-stressed trees soon after water application was renewed. Shoot elongation was reduced 25–30% for the 10-day period during and following drought and recovered thereafter to levels of non-stressed trees. Whole-tree ET_a was reduced by as much as 20% even following full recovery of the leaf level parameters, suggesting reduced canopy size and growth due to the stress period. Non-destructive, continuous (turgor pressure) and remotely sensed (canopy temperature) methods showed promising potential for monitoring effects of water stress, in spite of technological and data interpretation challenges requiring further attention.

1. Introduction

Irrigation increases yields by allowing greater fruit bearing capacity per tree and per land area and by allowing expansion of olive cultivation into regions too dry for rain-fed production (Fernández and Moreno, 1999; Ramos and Santos, 2009). While increasing fruit and oil yields, increased water application often has negative effects on olive oil quality parameters (Berenguer et al., 2006; Dag et al., 2008). Research trends indicate that maximization of yields while insuring high quality oil requires conditions of moderate water stress, at least during specific phenological stages (Ben-Gal et al., 2009). Optimization of irrigation is therefore expected to improve olive cultivation for oil production, while encouraging efficient use of scarce water resources. Methods for monitoring or recognizing plant water status and/or water stress conditions represent potentially powerful and important management tools for both mature, bearing olives, where management-induced water stress is expected to optimize oil yields and quality, and for olive trees in non-bearing growth stages for which maximum vegetative growth is of interest to growers.

Water status can be measured along the soil–plant–atmosphere continuum and can be quantified through direct measurement of soil and/or plant water status as well as by measuring indirect effects of the stress on plant parameters. Soil-based water status methods include sampling and gravimetric calculation of soil water, measures of soil water potential (tensiometers) and various probe-based methods for estimating volumetric soil water content (Jones, 2007).

* Corresponding author. Tel.: +972 8 9928644; fax: +972 8 9926485.
E-mail address: bengal@volcani.agri.gov.il (A. Ben-Gal).

0378-3774/$ – see front matter © 2010 Elsevier B.V. All rights reserved.
doi:10.1016/j.agwat.2010.08.008

Plant-based water status monitoring can involve direct measurements of physiological responses to water or can instead attempt to record changes in secondary processes indirectly affected by (usually less than optimal) water status. Plant response to water stress can be measured both at small scales (stem, leaf, parts of leaves), where physiological processes are affected and at the whole-tree-scale, where accumulative effects are evident. Small-scale monitoring includes the measuring of such parameters as xylem (sap) flow, stomatal conductance, photosynthesis, leaf temperature, and stem, leaf or fruit shrinkage (Jones, 2007; Naor, 2006). These provide an assessment of the physiological severity of water stress and contribute to the determination of threshold levels, as plants enter into, physiologically "shut down" due to, and recover from water stress. Physiological-based monitoring, however, does not permit quantification of cumulative effects. These include less than optimum growth, changes in phenological processes, and subsequent altered plant size and vegetative or reproductive production and must be considered at tree and orchard scales. Tree level quantification of water stress in both absolute and relative terms and its effects on growth, production and water consumption is vital for determining management strategies. Tree-scale information is also necessary for developing and utilizing transpiration driven growth models (De Wit, 1958) where reductions in actual evapotranspiration (ET_a) are related to corresponding reductions in biomass, canopy and yield.

Assessment of whole-tree responses to water stress, including cumulative effects on biomass and yield, can be aided by continuous determination of water balance components using lysimeters (Van Bavel, 1961; Hillel et al., 1969; Ben-Gal and Shani, 2002; Marek et al., 2006). Despite several disadvantages inherent to lysimeters, e.g., sidewall-boundary effects and microclimatic effects (Bergstrom, 1990; Flury et al., 1999; Corwin, 2000), they uniquely allow comparison of actual water and solute balance between different treatments under well-defined conditions. Weighing lysimeters additionally enable high temporal resolution (hours, days) quantification of ET rates. The information concerning water consumption, growth and production generated from lysimeter studies can be used to identify and quantify desirable management-induced water stress levels.

Since such whole-tree-scale monitoring is not practically feasible in commercial settings, the assessment of accessible, physiological-based measurements as indicators of water status can be valuable for managers and decision makers. The understanding of the physiological scale processes and responses in terms of whole-tree-scale effects of water stress will hopefully lead to practical and feasible field scale methods for management of desired water stress levels in olive trees.

The absolute values of measured water status are a function both of available water for uptake and transpiration, and of climatic conditions. In order to evaluate plant water status, and especially to use monitored water status data for irrigation scheduling, some type of normalization, either to non-stressed conditions or, preferably, to specific climate conditions, is necessary (Fernandez and Cuevas, 2010; Jones, 2004; Jones, 2007; Naor, 2006).

We have used drainage-weighing lysimeters to measure water balance components of non-bearing olives (*Olea europaea* cv Barnea) over a 3-month period including short-term events of controlled but severe water stress. The objective of the study was to use calculated actual tree-scale ET as a basis for evaluation of a variety of soil and plant-based water status and drought stress monitoring methods. Both conventional methods, such as stomatal conductance and stem water potential, and two novel methods under development, measuring leaf turgor pressure and canopy temperature, were evaluated.

2. Materials and methods

Single 2-year old 'Barnea' olive tree were planted in fifteen 2.5 m^3 volume free-standing lysimeters (Fig. 1) at the Gilat Research Center in the northwestern Negev, Israel (31°20′N, 34°40′E) in June 2008. The trees were irrigated daily, with quantities always exceeding (by ~20%) the previous day's transpiration rates as calculated from the weight data of the lysimeters. Nitrogen, phosphorus, potassium and micronutrients were added to the irrigation solution as liquid commercial 7:3:7 ($N:P_2O_5:K_2O$) fertilizer at a rate of 50 ppm N. Each lysimeter (Fig. 1) consisted of a polyethylene container (1.4 m high × 1.5 m diameter) filled with loamy sand soil, a bottom layer of highly conductive porous media (rockwool) in contact with the soil, and drainage piping filled with the same material extending downward from the lysimeter bottom. The rockwool drainage extension (Ben-Gal and Shani, 2002) disallowed saturation at the lower soil boundary while permitting water to move out of the soil and be collected. The lysimeter system included automatic water and fertilizer preparation and delivery and automatic drainage collection as described by Tripler et al. (2007). The soil surface in the lysimeters was covered by a water permeable geotextile (Non-Woven Geotextile, 500 g m^{-2}, Noam-Urim, Israel) to minimize evaporation losses. Individual lysimeters were positioned on square weighing platforms with load cells situated in each corner. By distributing load cell output current only over the relevant range of interest (4–5 tons) a resulting resolution of ±15.5 g was reached. ET was calculated daily according to: $ET = I - D - \Delta W$; where I is irrigation, D is drainage and ΔW is change in soil water. There was no rainfall during the experimental period.

The lysimeters were divided into three groups (Group 1, Group 2 and Group 3) of five trees. All trees received identical treatment from planting until the beginning of the current experiment. To study the effects of short-term stress, irrigation to each group of trees was withheld for a number of days during the summer of 2009. A preliminary stress round was conducted from the 4th to the 13th of June on Group 1. Based on the results from this stress

Fig. 1. Olive lysimeters at Gilat Research Center, Israel. Overview (left) and individual single tree weighing-drainage lysimeters (right).

period, along with estimations of anticipated changes in canopy size and climate demand, irrigation was withheld for 6 days for Groups 2 and 3, from July 23rd to July 28th, and from August 28th to September 2nd, respectively. Continuous monitoring included: meteorological data acquired from a weather station 200 m from the site, actual ET (ET_a) computed from the lysimeter water balance, and relative changes in leaf turgor pressure with leaf patch clamp pressure probes (Zimmermann et al., 2008). Reference ET (ET_0) was calculated according to the FAO Penman-Monteith equation for hourly time steps as described by Allen et al. (1998). In each period of drought and recovery, additional water status and water stress measurements were conducted daily between 12:00 and 14:00 local time on all trees. The "recovery" period refers to the time it took for all physiological parameters to return to the reference values or to stabilize on new values. The additional measurements included volumetric soil water content from time domain reflectometry (TDR) using a Tektronix 1502 cable tester (Tektronix Inc., Beaverton, OR, USA), stem water potential (ψ_{stem}) using a Scholander type pressure chamber (MRC, Israel), stomatal conductance (g_S) from a diffusion leaf porometer (SC-1, Decagon Devices, Inc., Pullman, WA, USA), canopy temperature (T_C) from thermal images acquired by an un-cooled infrared thermal camera (ThermaCAM model SC2000, FLIR systems), and quantum yield of photosystem II photochemistry (Φ_{PSII}) using a portable MINI-PAM photosynthesis yield analyzer (Heinz Walz GmbH, Effeltrich, Germany). Vegetative growth (shoot elongation) was measured during and after the stress period of Group 3. The daily monitoring continued after re-watering until full recovery was observed. In order to capture the diurnal behavior of the different parameters on both well-irrigated and drought-stressed trees, the measurements were augmented and conducted throughout the day on the day before re-watering (day of minimum available water, minimum ET and maximum water stress). Diurnal monitoring on these days started from before dawn (4:00) and continued until after dusk (20:00). A summary of the experimental setup and dates is given in Table 1.

Tree-based measurements were conducted on stems and leaves 0.5–1.5 m above the soil surface. Stem water potential was measured as described by Shackel et al. (1997) on single shoot endings with 6–7 leaves covered at least 2 h in advance by sealed aluminum–plastic bags. Shoot endings were taken from the northern (shaded) side of the trees' canopies. Stomatal conductance and fluorescence-based measurements were taken on young but fully grown leaves between 5 and 20 cm from the shoot tip. For each tree five samples, uniformly distributed over sun-exposed canopy, were taken. Shoot growth was measured by marking a point 20 cm from the tip of ten shoots equally distributed around each tree on the day that irrigation was discontinued for Group 3. Increase in shoot length was recorded on the 10th and 20th day following.

The efficiency of photosystem II photochemistry was determined by computing Φ_{PSII} according to the relationship: $\Phi_{PSII} = (F'_m - F_t)/F'_m$, where F'_m is maximum fluorescence when applying a saturation flash to a light-adapted leaf; and F_t is the level of fluorescence immediately before saturation flash (Maxwell and Johnson, 2000).

Leaf patch clamp pressure probes (LPCP probes) were used to monitor relative changes in leaf turgor pressure. Three trees in each group were each equipped with single LPCP probes, located inside the canopy to avoid direct sunlight. The principle of the probe is fully explained in Zimmermann et al. (2008) and Westhoff et al. (2009). In short, two magnets were used to apply a constant known pressure to a young fully developed leaf and to sense the pressure passing through the leaf. The magnitude of the sensed pressure depends on a turgor-independent, constant term (arising from the compression of the cuticle, air-filled spaces, cell walls and the silicone of the probe) and turgor pressure. Thus, if the external pressure is kept constant and an equilibrium value has been reached after clamping, the difference between the exerted and the sensed pressure only depends reciprocally on turgor pressure (Zimmermann et al., 2008). Probe output pressure values decrease to minimum values at nighttime when turgor is highest and increase during the day with the diminishing of turgor in leaves. Under less than optimum water conditions, both maximum and minimum output pressure increase, indicating lower daytime turgor pressure and less nighttime recovery, respectively. An example of a time course for a single probe before, during, and after a drought event is shown in Fig. 2. We used the calculated area under daily time course curves of probe pressure readings (PPA), as highlighted in the figure, to give a relative quantification of turgor-related water stress. PPA data during drought and recovery periods were normalized to non-stressed values and taken as 100% on the day immediately prior to drought initiation.

Thermal images were taken 2 m above the canopy of individual trees. Each image contained a wet reference to aid in normalizing temperature to climatic conditions. The images were used to determine both absolute average canopy temperature and climate-normalized crop water stress index (CWSI; Jones, 1992) for each tree, according to the methodology described by Ben-Gal et al. (2009).

Statistical variance, regression and correlation analysis was aided by JMP (SAS Institute Inc., Cary, NC, USA), SPSS 15.0.1 for Windows (SPSS Inc., Chicago, IL, USA) and SigmaPlot 10.0 (Systat Software, San Jose, CA, USA).

Table 1
Summary of drought periods and measurements taken. Whole-tree evapotranspiration rate (ET_a), stem water potential (ψ_{stem}), stomatal conductance (g_S), area under daily pressure probe data (PPA), quantum yield of photosystem II photochemistry (Φ_{PSII}), canopy temperature (T_C), crop water stress index (CWSI), and shoot elongation (shoot length).

Group under stress	1	2	3
Designation	Preliminary	July	August
Date irrigation discontinued	04 June	23 July	28 August
Date irrigation renewed	14 June	29 July	03 September
Date of diurnal measurements	–	28 July	02 September
Measurements taken			
ET_a	+	+	+
ψ_{stem}	+	+	+
g_S	+	+	+
PPA	+	+	+
Φ_{PSII}	–	–	+
T_c and CWSI	–	–	+
Shoot length	–	–	+

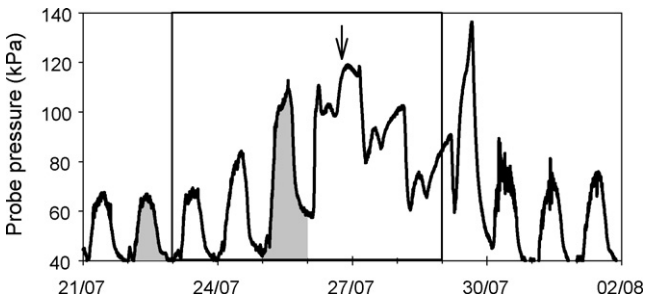

Fig. 2. Raw data from a single leaf clamp pressure probe on a tree in Group 2. Period of ceased irrigation is enclosed by a block. Examples of area under the graph for single days (PPA) are shadowed for a day with full irrigation (22 July) and on the third day without irrigation (25 July). The arrow represents reaching conditions of apparent near-zero turgor and onset of inversed diurnal probe output data.

3. Results

3.1. Evapotranspiration and growth

Reference ET (ET_0, Fig. 3A) averaged ~10 ± 1 mm day^{-1} from the beginning of the experimental period until mid-August. From mid-August till the end of the experimental period, ET_0 declined linearly and reached ~7 mm day^{-1} at the end of September. Whole-tree ET (ET_a) was calculated daily using water balance over the entire experimental period, starting in June and continuing through the end of September 2009. Fig. 3B depicts average daily ET_a for each of the three groups. Evapotranspiration increased over time with dips apparent during the stress periods. Also visible in Fig. 3B are a 3-day period from 30 June–1 July with particularly high ET_a reflecting particularly high ET_0 (Fig. 3A) and a slight dip at the beginning of August when problems with the irrigation system caused delayed irrigation events and several days of reductions in ET_a of all the groups. During their respective drought periods, Group 2 and Group 3 exhibited nearly identical patterns of reduction in ET_a. After a recovery period of 4 days, a permanent decrease in the ET of the stressed trees was evident compared to non-stressed trees. Group 1 experienced relatively slight stress in June's preliminary drought period which caused a visible, but non-significant retardation in ET_a at the early stage of the experiment. The ET_a of Group 1 was not permanently affected and returned to that of non-stressed trees during the subsequent months. Daily values of ET_a for Group 1 nearly tripled over the course of the summer, from just over 30 L tree^{-1} to more than 80 L tree^{-1}. Maximum values of daily ET_a for Groups 2 and 3, which experienced more severe water stress during their respective drought periods, were significantly lower than those of Group 1 and reached approximately 70 L tree^{-1}. Evapotranspiration for all the groups stopped increasing towards the end of August and began to decline after the final stress period in mid-September.

Actual ET as seen in Fig. 3B was a function of canopy size and environmental evaporative demand in addition to water availability. In order to aid interpretation of the data and to facilitate subsequent discussion, the ET_a data have been manipulated in two different ways in Fig. 3C and D. First, ET_a was accumulated over the course of the experimental period. Total average accumulated ET_a per tree (Fig. 3C) was around 3200 L for all groups at the beginning of the summer. This number is the sum of daily tree-scale ET_a starting from the planting of the trees in June 2008. Deviations of the patterns of accumulated ET_a over the course of the summer of 2009 (Fig. 3C) were evident during and following the drought periods.

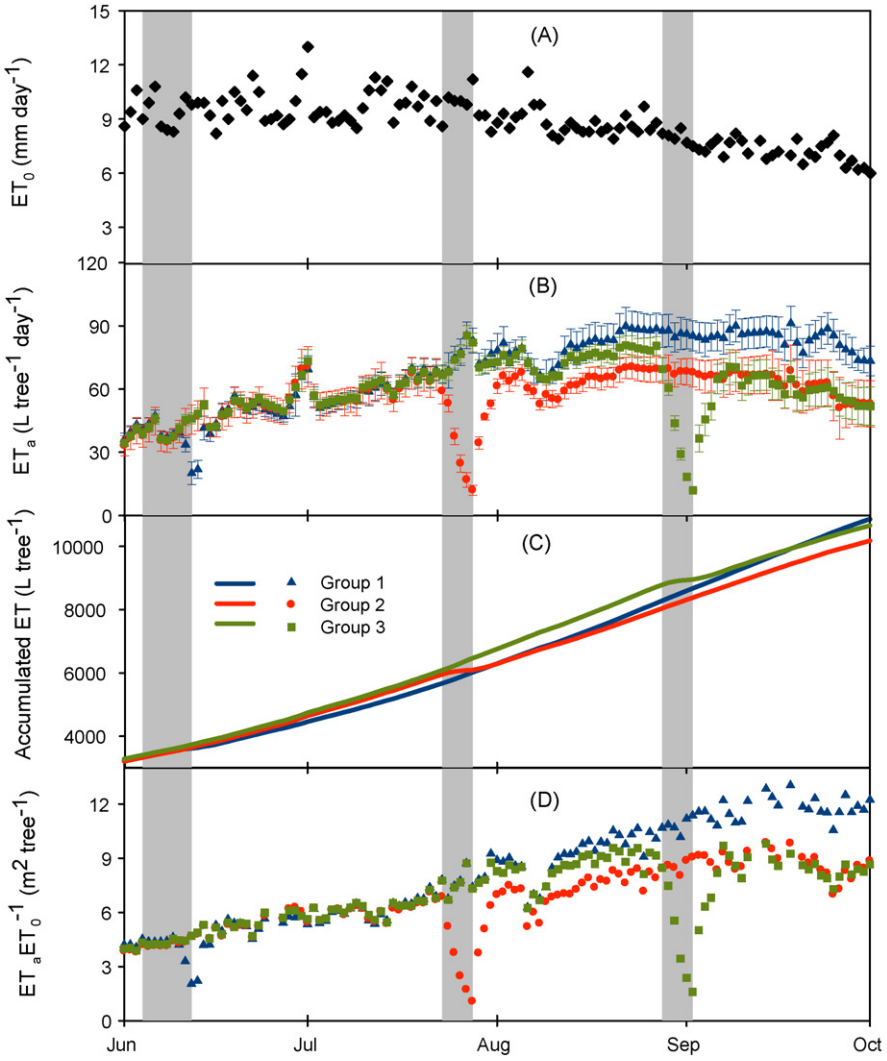

Fig. 3. Evapotranspiration (ET) over the time course of summer 2009 including drought periods. Periods of discontinued irrigation are shown as gray horizontal bars for Groups 1, 2 and 3, left to right, respectively. Symbols are averages and error bars standard deviation, $n = 5$. (A) reference evapotranspiration (ET_0), (B) daily actual tree-scale evapotranspiration (ET_a), (C) accumulated average ET_a (measurements began from time of planting in lysimeters: July 2008), and (D) effective transpiring canopy area (m^2/tree) calculated by normalizing actual ET with reference ET (ET_a/ET_0).

During drought periods the decreased ET_a resulted in lower total accumulated ET_a, and decreases were also found in the slopes of the curves in Fig. 3C following each group's period of drought. Following the drought period to Group 2 (11 July–01 September) the slope of its accumulated ET_a curve was 66.1 L tree^{-1} day^{-1} compared to 72.3 and 72.1 L tree^{-1} day^{-1} for Groups 1 and 3 respectively. Following the drought period for Group 3 (14 September–01 October) its slope was 55.5 L tree^{-1} day^{-1} while that of the control (Group 1) was 69.9 L tree^{-1} day^{-1}. The second manipulation was computing the average effective transpiring canopy size of the individual trees (m^2 tree^{-1}), calculated by dividing ET_a (L tree^{-1} day^{-1}) by ET_0 (mm day^{-1} = L m^{-2} day^{-1}) (Fig. 3D). Changes in effective transpiring canopy size reflect tree growth as long as transpiration is not limited by water availability or some other stress-causing factor. Apparent reductions during periods where irrigation was stopped are obvious, as is a slight dip at the beginning of August during the short period of reductions in ET_a of all the groups due to system malfunction and delayed irrigation events. The effective transpiring canopy area increased for all groups throughout the period up until mid-September, when it more or less stabilized. Starting at around 4 m^2 tree^{-1}, effective transpiring canopy areas of non-stressed trees reached more than 11 m^2 tree^{-1} by the end of the summer while the trees of Groups 2 and 3, experiencing the pronounced drought periods, reached a maximum of 9 m^2 tree^{-1}.

Fig. 4 provides a look at the dynamics of climate (ET_0), soil water, and ET_a during the drought and re-irrigation periods. Diurnal patterns of ET_0 (in units of mm h^{-1}) are displayed for the two periods in Fig. 4A. In the figure, the greater climate demand in the July compared to the August period is evident in the slightly longer day length with positive ET_0 and significantly greater peak rates. Soil water content measured at four depths in two individual lysimeters from 26 August till 6 September is shown in Fig. 4B. Volumetric soil water content in the upper layers of the well-watered lysimeter fluctuated from ~20% immediately following irrigation to less than 10% prior to the daily irrigation events. Lower soil layers showed similar wetting and drying patterns with smaller fluctuations. The soil water content of the lysimeter subjected to drought, which was identical to that of the well-watered lysimeter prior to stopping daily irrigations, declined to 5–10% after 1 day of drought and to 2–6% on the ultimate day of drought, after 6 days without irrigation. During the drought period, volumetric water content was lower in the upper soil layers compared to closer to the bottom of the lysimeter. Tree-scale hourly ET_a rates calculated from lysimeter water balance are shown in Fig. 4C for both the "July" (23 July–3 August) period when Group 2 trees were induced to water stress and for the "August" (26 August–6 September) period when Group 3 trees experienced drought. Daily patterns for both well-watered and drought-stressed trees were remarkably similar during the two periods. Rates and patterns of ET_a were unaffected on the first day irrigation was discontinued and reduced steadily thereafter. On the second and third days following, the non-irrigated trees followed the same daily parabolic curves as the non-stressed trees, but with lower peaks. From the fourth day, peak ET_a rates shifted to earlier in the day. Midday decreases in ET_a were found for stressed trees and for the well-watered trees in July. The midday reductions began earlier and lasted for a longer time compared to those in well-watered trees during the stress period and the first few days after re-irrigation during the recovery period. Rates of ET_a increased to stable values following re-introduction of irrigation, but to levels lower than those of continuously irrigated trees. We used the data from Fig. 4 to compare water consumption calculated from the soil-based TDR monitoring to the water balance ET_a calculations for the non-irrigated trees. Rough calculation of water in the root zone from the TDR data (approximate total soil volume of 2 m^3 and decrease of depth averaged volumetric water content from 15% to 4%) indicated a loss of around 220 L. Accumulated ET loss during the same period (integral of the area under the ET_a curves in Fig. 4B) was 203 L for Group 2 and 232 L for Group 3.

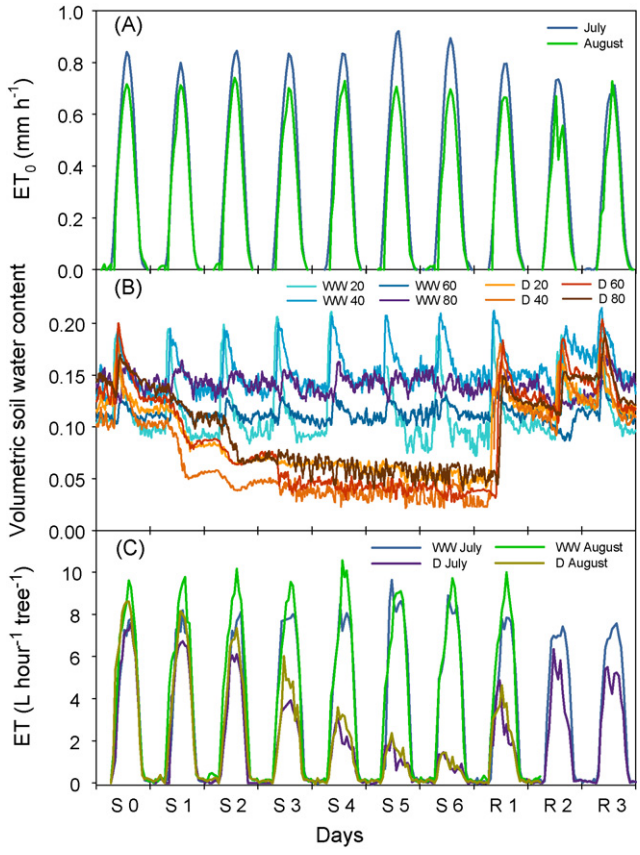

Fig. 4. Hourly reference evapotranspiration (ET_0) rates for both stress periods (A), soil water from TDR measured at 4 depths (20, 40, 60 and 80 cm from soil surface) (B), measured during 26 August–06 September; and evapotranspiration (ET) (C), going into and coming out of stress periods. The *X*-axis is days of stress (S) and recovery (R) for Group 2 (23 July–03 August; indicated as "July") and for Group 3 (26 August–06 September; indicated as "August"). WW stands for well-watered lysimeters and D for lysimeters subjected to drought. ET values are average rates for five trees. TDR values are from individual probes in representative irrigated and non-irrigated lysimeters.

The apparent decelerated canopy growth rates found in the whole-tree ET_a values (Figs. 3 and 4) during and following drought periods were also evident in shoot growth measurements. Shoot length was measured 1 day before irrigation to Group 3 was discontinued (27 August) and elongation was measured after 10 days and again after 20 days. Analysis with one way ANOVA and Tukey–Kramer all pairs test showed significantly less growth for Group 3 (2.3 cm) compared to Groups 1 and 2 (3.7 and 3.3 cm, respectively) for the 10-day period including the water stress and recovery. For the next 10-day period, shoot growth in Group 3 (2.2 cm) no longer statistically differed from Groups 1 and 2 (2.8 and 2.4 cm, respectively).

3.2. Water status and stress monitoring

Differences between irrigated and non-irrigated trees were visible from the first or second day of stress and all parameters returned to levels corresponding to those of the well-watered trees values within 4 days after resuming irrigation (Fig. 5). On the sixth and final day without irrigation, when the trees were under severe stress with ET_a less than 0.15 of irrigated trees and very little remaining available water in the soil (Fig. 4), visible leaf curling became evident.

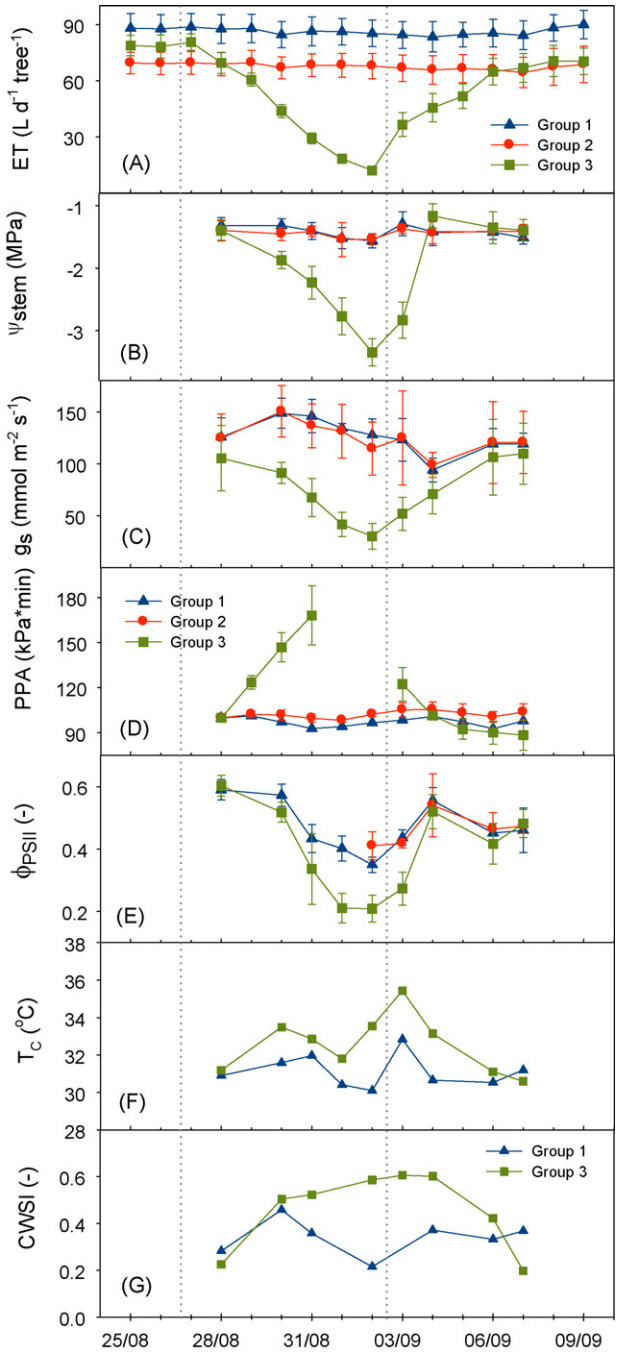

Fig. 5. Midday measurements going into and recovering from drought. Stress period for Group 3, August 2009. (A) whole-tree evapotranspiration (ET), (B) stem water potential (ψ_{stem}), (C) stomatal conductance (g_S), (D) area under daily values from leaf clamp pressure probe data (PPA), (E) quantum yield of photosystem II photochemistry by fluorometer (Φ_{PSII}), (F) canopy temperature (T_C), (G) crop water stress index (CWSI). Dotted vertical lines indicate beginning and end of drought period. Symbols are averages and error bars standard deviations, $n = 5$.

The patterns of response of ET_a, ψ_{stem}, g_S, and PPA were similar for the drought periods of both Groups 2 and 3 and we therefore present them together while including data graphically from only the second period. Well-watered trees had average daily ET_a ranging from 70 to 90 L tree^{-1} during the July period and from 80 to 90 L tree^{-1} during the August period. Their midday average ψ_{stem} values ranged from −1.4 to −2 MPa in the first period and −1.3 to −1.4 MPa in the second and their corresponding average midday g_S rates were 90–125 mmol m^{-2} s^{-1} in the first period and 90–150 mmol m^{-2} s^{-1} in the second. On the first day of drought the differences between irrigated and non-irrigated groups were not yet significant. On the second and third day the ET_a of non-irrigated trees dropped about 10% per day, and decreased to about 30% of that of irrigated trees on the fourth day. ET_a continued to decrease to a low of 14% on the sixth day of stress, after which irrigation was resumed (Fig. 5A). Similar to the ET, decreases in ψ_{stem} sharpened after 2 days (Fig. 5B). ψ_{stem} values continued to decrease, to lows of around −3.5 MPa on the last days of stress. Midday g_S of non-irrigated trees behaved virtually identically to daily ET_a, and reached low points of ∼30 mmol m^{-2} s^{-1} on the last days of stress (Fig. 5C). ET_a stabilized after 3–4 days following resumption of irrigation but remained lower than that of the continuously irrigated groups. Stem water potential recovered completely within 1 day following re-irrigation while g_S recovered to non-stress values on the third day of re-irrigation.

The leaf patch clamp pressure probe raw data (Fig. 2) indicated lower daytime turgor and only partial nighttime recovery to full turgor on the second day after cessation of irrigation. The area below daily curves from the pressure clamp probes (PPA, Fig. 5D) correlated well with ET and the other measurements, increasing during the drought period and decreasing during recovery. The diurnal patterns of the pressure clamp probes inversed under severe stress levels on the fifth and sixth days of stress during both periods (see arrow in Fig. 2), rendering PPA values for those days meaningless. After reinstating irrigation PPA values returned to non-stress levels within 1 day, simultaneously with ψ_{stem}.

The fluorescence-based Φ_{PSII} (Fig. 5E) of non-irrigated trees decreased to significantly lower values than those of irrigated trees after 4 days. The low point for Φ_{PSII} was reached after 5 days and did not decrease further on day 6. Φ_{PSII} recovered simultaneously with ψ_{stem}. Canopy temperature and CWSI (Fig. 5F and G, respectively) also reflected the effect of drought with higher leaf temperatures causing higher CWSI values from the second day of drought. On the fourth day of recovery the drought-stressed trees returned to T_C and CWSI values similar to those of the well-watered trees.

Diurnal measurements for water status monitoring are found in Fig. 6 (Group 3 on sixth day without irrigation). The measurements of ψ_{stem} and g_S closely follow those of ET_a throughout the day. Evapotranspiration was negligible in the night and, along with ET_0, followed parabolic curves during the day peaking between 12:00 and 14:00. The diurnal patterns for the July period (Group 2 on sixth day without irrigation, data not shown) for ET_a, ψ_{stem}, g_S, and PPA were similar to those shown for the second period in Fig. 6 with a number of climate-related differences apparent. Daylight ET_0 (area under relevant curve in Fig. 6A) was 2 mm higher on 26 July as compared to 3 September. Corresponding differences were found for ψ_{stem} and g_S measurements in irrigated trees; ψ_{stem} decreased to −2 MPa on 26 July, whereas on 3 September it did not fall below −1.5 MPa, and a midday dip in g_S was evident on 26 July and not on 3 September. The ET_a and g_S of the stressed trees slightly increased above nighttime values in the mornings, reaching peak values between 8:00 and 10:00 and decreasing at noon (Fig. 6A and C). Similarly, ψ_{stem} decreased from maximum nighttime values during the day (Fig. 6B). Significant differences between irrigated and non-irrigated trees were found throughout the day for ψ_{stem} and from 7:00 to 7:30 until at least 18:00 for ET_a and g_S. Absolute values of ET_a and g_S were similar for the non-irrigated trees on the two dates, ranging, respectively, from 0 to 9 L h^{-1} tree^{-1} and from 25 to 140 mmol L^{-1} s^{-1}. Nighttime ψ_{stem} of stressed trees was lower (<2.5 MPa) on 26 July compared to 3 September (<2.0 MPa). Daytime ψ_{stem} of the non-irrigated trees fell to around −3.5 MPa on both days and remained fairly stable between 10:00 and 15:00. Φ_{PSII} (Fig. 6D) showed significant differences between irrigated and non-irrigated trees between 9:00 and 16:00 on 3 September. Similarly T_C and CWSI (Fig. 6E and F) showed significant differences

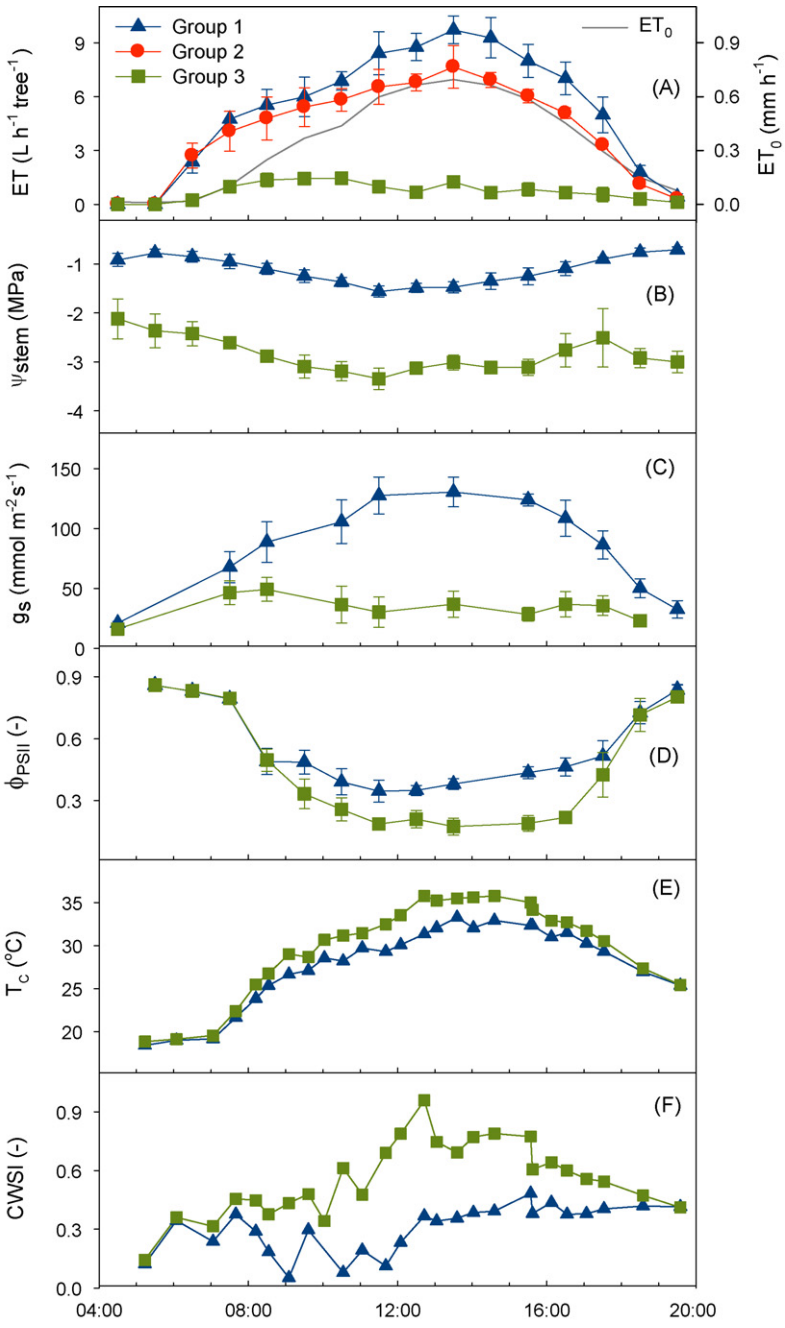

Fig. 6. Diurnal measurements for well-watered (Groups 1 and 2) and drought-stressed (Group 3) olive trees on September 2, 2009. (A) whole-tree evapotranspiration (ET), (B) stem water potential (ψ_{stem}), (C) stomatal conductance (g_S), (D) quantum yield of photosystem II photochemistry by fluorometer (Φ_{PSII}), (E) canopy temperature (T_C), (F) crop water stress index (CWSI). Symbols are averages and error bars standard deviations, $n = 5$.

between irrigated and non-irrigated trees, with largest differences around midday and more pronounced differences in CWSI than in T_C.

Significant correlations were found between whole-tree daily ET rates and midday values of ψ_{stem}, $g_{S,}$ Φ_{PSII}, and PPA for the data sets entering into and recovering from drought (Table 2). Midday canopy temperature and CWSI were less but still significantly correlated with daily whole-tree ET.

4. Discussion

The behavior of groups of drought-exposed trees during the July and August periods of ceased irrigation was coincidentally identical. The trees had a given, fixed, root zone volume of approximately 2 m^3 of soil, dictated by the lysimeter containers. Thus at the start of a drought experiment there was a fixed amount of water in the soil which could be depleted. The rate of ET_a (Figs. 3B and 4C), and therefore the rate of depletion of soil water (Fig. 4B), was dependent upon climate demand and tree size. In Group 2's period of drought, the climate demand was higher than in Group 3's (~10.0 mm day^{-1} compared to ~8.0 mm day^{-1} ET_0) but this was compensated by the fact that the trees had grown during the month between the drought periods. Therefore, continuously well-irrigated trees had effective transpiring canopy areas (Fig. 3D) that were some 40% larger (10 m^2 compared to 7 m^2) at the start of the Group 3's stress period compared to the beginning of the Group 2's. The contingent

Table 2
Regression coefficient (r^2) values between the water stress indicators for daily measurements going into and recovering from drought: whole-tree evapotranspiration (ET_a), stem water potential (ψ_{stem}), stomatal conductance (g_S), quantum yield of photosystem II photochemistry (Φ_{PSII}), canopy temperature (T_C), crop water stress index (CWSI) and area under daily pressure probe data (PPA).

	ET_a		Ψ_{stem}		g_S		Φ_{PSII}		T_C		CWSI	
Ψ_{stem}	0.69	***										
g_s	0.72	***	0.58	***								
Φ_{PSII}	0.65	***	0.63	***	0.49	***						
T_C	0.46	**	0.5	**	0.56	**	0.34	*				
CWSI	0.38	*	0.25	ns	0.33	*	0.23	ns	0.55	**		
PPA	0.59	***	0.3	***	0.26	**	0.26	*	0.13	ns	0.17	ns

ns = not significant.
* $P \leq 0.05$.
** $P \leq 0.01$.
*** $P \leq 0.001$.

consequence of this was that absolute values of ET_a and the rate of soil water depletion were virtually identical in both experimental periods.

The short-term periods of drought decreased vegetative growth. This was apparently true even for Group 1 that experienced only a relatively mild stress in the preliminary experiment in June. While Group 1's ET_a rates after recovery were not significantly different from the other groups, patterns of accumulated ET implied smaller trees and smaller growth rate following the preliminary drought period. The growth rate of the young trees during the summer of 2009 was fairly remarkable. Climate-normalized ET-based calculations ($ET_a ET_0^{-1}$: Fig. 3D) indicate that non-stressed trees nearly tripled their canopy area between June and October. The canopy growth driven increase in ET stopped towards the middle of September, after which the transpiration stabilized around a fixed fraction of climatic demand (ET_0, Fig. 3D).

The single episodes where available soil water was nearly completely depleted caused long-term significant decreases of more than 20% in transpiration rates and in the effective transpiring canopy of individual trees. This impairment of whole-tree transpiration following the periods of drought was not reflected in any of the leaf or canopy-based measurements, all of which recovered to the values of trees that did not experience stress within a number of days following re-irrigation. This supports the claim that long-term reduction of ET_a was due simply to reduced growth during the drought itself and to the subsequent lower growing capacity of the smaller trees. Similar reductions in vegetative growth were reported in field experiments by Greven et al. (2009) for a 3-month drought period on 'Verdale' olives in New Zealand and by Iniesta et al. (2009), for 2 years of continuous deficit irrigation of 'Arbequina' olives in Spain. Shoot growth was also found to be highly sensitive to drought by Sofo et al. (2008) who compared dry weights of shoots in rain-fed and irrigated 'Coratina' olives in Spain over a 7-year period. In that study partial inhibition of shoot growth was reported at pre-dawn leaf water potentials as high as −1 MPa, and severe inhibition was found at pre-dawn leaf water potentials below −1.3 MPa.

All the measured parameters were sufficiently sensitive to conditions causing lower than optimal water consumption and therefore are potentially useful for monitoring water status (Table 2, Fig. 5). The coincidental similarity in development into and recovery from stress experienced by Groups 2 and 3 made direct comparison of day by day response of physiological parameters possible and aided in correlating between the various methods. Positive correlations were found for the data set representing the midday values for all the trees entering into and recovering from drought stress (Table 2). It is obvious from Fig. 5 that the methods are all better correlated for the period entering into stress compared to the period of recovery where ψ_{stem} and PPA return to non-stressed levels faster than the other parameters.

Entrance into stress (reduction of ET_a) was identified by significant differences between midday measurements of irrigated and non-irrigated trees for ψ_{stem}, g_S, T_C, and CWSI. The fluorescence-based photosynthesis calculations were slightly less sensitive to induction of water stress as they showed significant differences a day later. Recovery following the stress was also successfully portrayed by all the methods, each of which was returned to non-stressed values. ψ_{stem}, PPA and Φ_{PSII} fully recovered after 2 days of irrigation while gs and the canopy temperature-based measurements more closely followed ETa and returned to steady high values after 4 days.

The turgor-related PPA measurements in response to stress were relatively insensitive to climate and gave the same level of response during the two drought periods. Changes in PPA entering into drought were highly pronounced compared to the other parameters, substantiating that turgor is particularly sensitive to changes in water potential of the soil (Hsiao, 1973). This was also reported by Sofo et al. (2008) who found onset of partial and severe inhibition of turgor pressure at pre-dawn leaf water potentials of −1 and −3.2 MPa respectively in 'Coratina' olives planted in pots. For mild to moderate stress levels in particular, PPA seems an appropriate measure for water status, especially since the method is non-invasive, continuous and automatic. At near-zero turgor the assumptions leading to a sensor's constant term were apparently no longer valid and the resulting calculated PPA from output values was meaningless, but this effect was reversible. Upon re-watering, increased relative turgor pressure was measured as seen by the return to the accustomed profiles of the probe output pressures and to pre-stress levels of calculated PPA. Normally, such severe stress levels and zero leaf turgor pressure values would not be considered desirable and therefore their measurement is likely not necessary for monitoring and water management purposes.

Absolute values of the other physiological-related monitoring methods were affected by climate as well as by water status and were therefore different for the two periods. The values of measured stomatal conductance were particularly influenced by climate. Measurements from irrigated trees demonstrate that g_S in the first period, with a higher climatic evaporative demand, was only around 120 mmol m^{-2} s^{-1} compared to 150 mmol m^{-2} s^{-1} in the second period. These numbers are lower than those reported for well-watered trees by Pérez-López et al. (2008) (190 mmol m^{-2} s^{-1}) and Giorio et al. (1999) (240 mmol m^{-2} s^{-1}). The g_S of severely drought-stressed trees, ~30 mmol m^{-2} s^{-1} during both stress periods in the current study, were equivalent to those reported for drought-stressed trees in the previously mentioned studies. Stem water potential was also affected by climate, although less pronounced than stomatal conductance. The effect of climate on ψ_{stem} decreased as the level of stress increased.

Stomatal conductance was previously found to be correlated with stem water potential of olive trees (Ben-Gal et al., 2009; Fernandez et al., 2006; Tognetti et al., 2005, 2007; Pérez-López

et al., 2008; Giorio et al., 1999) and of other deciduous fruit trees (Naor, 2006). Greven et al. (2009) found low correlation between stomatal conductance and stem water potential, but were working with more severely stressed trees with stem water potentials of −4 MPa. Stomata are all but closed at −2.5 MPa in many fruit trees (Naor, 2006). We found that transpiration and photosynthesis continued for olives, albeit at reduced rates and with diurnal patterns shifting to the morning hours, at stem water potential as low as −3.5 MPa. Others have suggested that this is true at potentials as low as −6 MPa (Sofo et al., 2008) or even −10 MPa (Guerfel et al., 2009).

Fluorescence-based measurements are generally understood to represent particularly sensitive elements of the photosynthesis system (Maxwell and Johnson, 2000). The fact that Φ_{PSII} responded slower than other parameters as drought was introduced supports the suggestion that olives have mechanisms to prolong maintenance of photosynthesis under stress-causing conditions (Sofo et al., 2008). The measured maximum Φ_{PSII} of 0.86 at pre-dawn agrees with the maximum Φ_{PSII} of 0.83 found in most species (Maxwell and Johnson, 2000). Quick recovery in photosynthetic efficiency was also observed by Sofo et al. (2008), who found that photosynthesis recovered even faster than leaf water potential.

Canopy temperature was found to be significantly correlated with ET, ψ_{stem}, g_S, and $\Phi_{PSII,}$ and the CWSI to all except for ψ_{stem} and Φ_{PSII}. Ben-Gal et al. (2009) showed good correlation between canopy temperature and CWSI and soil water, stem water potential, and stomatal conductance in mature 'Barnea' olive trees grown under various levels of sustained deficit irrigation in a commercial orchard using images of individual trees. Sepulcre-Cantó et al. (2006) found similar correlations for stem water potential and T_C from airborne images of entire orchards. The somewhat weaker correlations of the CWSI (compared to correlations to T_C) imply that the normalization procedure, originally developed for field crops, is not as effective for olive trees and might benefit from adaptation.

The diurnal measurements confirm that around midday water stress is most obvious, showing largest differences between stressed and non-stressed trees. Under severe stress levels diurnal patterns of transpiration, stomatal conductance, and photosynthesis related measurements shift, with highest values occurring during the early hours of the day.

Because of their dependence on climate, the absolute values of the physiological measures are of little value for monitoring water status except at levels of severe stress (Fernandez and Cuevas, 2010; Jones, 2007). To be more useful, the data must be compared to measurements from non-stressed trees or must be somehow normalized to climate. Climate-normalization is common for transpiration, where ET_0 and crop coefficient values are used to compute potential transpiration. This is also the case for CWSI where canopy temperature is normalized to a climate-determined theoretical range of leaf temperatures. A similar normalization would be useful for parameters such as stomatal conductance and stem water potential.

An alternative to compensate for the influence of climate is by continuous monitoring, where measurements can be compared to themselves and trends analyzed over time to benefit water management decision making. This is basically what is done in the turgor-related PPA measurements, where increases compared to 'normal' indicate onset of stress. Additional plant-based monitoring methods with potential for continuous measurements and similar data analysis and utilization are sap flow (Fernández et al., 2008; Greven et al., 2009) and trunk or stem size (Moriana and Fereres, 2002; Fernandez and Cuevas, 2010). Higher reliability may possibly be achieved by combining methods (Fernandez and Cuevas, 2010).

Under field conditions, the soil volume available for individual trees is likely to be larger than that in the lysimeters of this experiment. A larger buffer for root available water would likely reduce the intensity of response to drying conditions and possibly give the tree time to apply physiological drought response mechanisms. The results from this study were from not yet fruiting young olive trees with very high vegetative growth rates. Use of the tested methods for stress avoidance management is therefore applicable in young non-bearing orchards and in orchards in non-reproductive phenological stages where high vegetative growth rates are desirable. The findings need to be confirmed and calibrated with fruit bearing trees as well. Several differences are expected for bearing trees. Firstly, that both water consumption and vegetative growth will vary as a function of crop load (Dag et al., 2010). And secondly, since water status will affect quality as well as yield (Dag et al., 2008), that some level of water stress at certain phenological stages will be desirable to optimize oil production. The methods are therefore expected to become relevant for mature olive orchards to aid in maintaining target stress levels. These will, however, first need to be determined quantitatively and cumulatively on the whole-tree-scale, in order that they can be translated into physiological water stress management targets defining water stress duration and severity.

5. Conclusions

Drought lead to complete utilization of plant-available water in soil of lysimeters and to substantial decreases in physiological processes, but not to their complete shut down. In young olives, a one-time drought event with near total soil water depletion lasting only 6 days lead to permanent significant reductions in whole-tree evapotranspiration rates and apparent tree size. All tested methods for direct and indirect monitoring responses to drought were successful in recording entry into and exit out of short-term severe water stress. Leaf and stem-based hand measured stem water potential, stomatal conductance, and fluorescence-based photosynthesis estimations were particularly well correlated with whole-tree actual ET. These results represent a first step in determining thresholds for desired water status in olive trees, measurable by physiological, small-scale monitoring, including considerations of whole-tree and long-term water stress effects. To complete this, continued work on trees in fruit bearing stages is necessary. Ease and/or expense of each monitoring method obviously influence its potential for ultimate adoption as a management tool. For this reason, and in spite of remaining technological and data interpretation challenges, remotely sensed canopy temperature-based monitoring and methods that can be made continuously, like the leaf patch clamp pressure probe, seem promising and deserve further development and investigation.

Acknowledgement

The building and maintaining of the lysimeter facility was supported generously by the JCA Charitable Foundation (ICA Israel).

References

Allen, R.G., Pereira, L.S., Raes, D., Smith, M., 1998. Crop evapotranspiration: guidelines for computing crop water requirements Irrig. Drain. Paper 56. UN-FAO, Rome.

Ben-Gal, A., Shani, U., 2002. A highly conductive drainage extension to control the lower boundary condition of lysimeters. Plant Soil 239, 9–17.

Ben-Gal, A., Agam, N., Alchanatis, V., Cohen, Y., Yermiyahu, U., Zipori, I., Presnov, E., Sprintsin, M., Dag, A., 2009. Evaluating water stress in irrigated olives: correlation of soil water status, tree water status, and thermal imagery. Irrig. Sci. 27, 367–376.

Berenguer, M.J., Vossen, P.M., Grattan, S.R., Connell, J.H., Polito, V.S., 2006. Tree irrigation levels for optimum chemical and sensory properties of olive oil. HortScience 41, 427–432.

Bergstrom, L., 1990. Use of lysimeters to estimate leaching of pesticides in agricultural soils. Environ. Pollut. 67, 325–347.

Corwin, D.L., 2000. Evaluation of a simple lysimeter-design modification to minimize sidewall flow. J. Contam. Hydrol. 42, 35–49.
Dag, A., Ben-Gal, A., Yermiyahu, U., Basheer, L., Nir, Y., Kerem, Z., 2008. The effect of irrigation level and harvest mechanization on virgin olive oil quality in a traditional rain-fed 'Souri' olive orchard converted to irrigation. J. Sci. Food Agr. 88, 1524–1528.
Dag, A., Bustan, A., Avni, A., Tzipori, I., Lavee, S., Riov, J., 2010. Timing of fruit removal affects concurrent vegetative growth and subsequent return bloom and yield in olive (*Olea europaea* L.). Sci. Hortic. 123, 469–472.
De Wit C.T., 1958. Transpiration and crop yield. Versl. Landbouwk. Onderz. 64.6 Inst. of Biol. and Chem. Res. on Field Crops and Herbage, Wageningen, The Netherlands.
Fernández, J.E., Moreno, F., 1999. Water use by the olive tree. J. Crop Prod 2, 101–162.
Fernandez, J.E., Diaz-Espejo, A., Infante, J.M., Duran, P., Palomo, M.J., Chamorro, V., Giron, I.F., Villagarcia, L., 2006. Water relations and gas exchange in olive trees under regulated deficit irrigation and partial rootzone drying. Plant Soil 284, 273–291.
Fernández, J.E., Green, S.R., Caspari, H.W., Diaz-Espejo, A., Cuevas, M.V., 2008. The use of sap flow measurements for scheduling irrigation in olive, apple and Asian pear trees and in grapevines. Plant Soil 305, 91–104.
Fernandez, J.E., Cuevas, M.V., 2010. Irrigation scheduling from stem diameter variations: A review. Agr. Forest Meteorol. 150, 135–151.
Flury, M., Yates, M.V., Jury, W.A., 1999. Numerical analysis of the effect of the lower boundary condition on solute transport in lysimeters. Soil Sci. Soc. Am. J. 63, 1493–1499.
Giorio, P., Sorrentino, G., d'Andria, R., 1999. Stomatal behaviour, leaf water status and photosynthetic response in field-grown olive trees under water deficit. Environ. Exp. Bot. 42, 95–104.
Greven, M., Neal, S., Green, S., Dichio, B., Clothier, B., 2009. The effect of drought on water use, fruit development and oil yield from young olive trees. Agr. Water Manage. 96, 1525–1531.
Guerfel, M., Baccouri, O., Boujnah, D., Chaïbi, W., Zarrouk, M., 2009. Impacts of water stress on gas exchange, water relations, chlorophyll content and leaf structure in the two main Tunisian olive (*Olea europaea* L.) cultivars. Sci. Hortic. 119, 257–263.
Hillel, D., Gairon, S., Falkenflug, V., Rawitz, E., 1969. New Design of a low-cost hydraulic lysimeter system for field measurement of evapotranspiration. Isr. J. Agric. Res. 19, 57–63.
Hsiao, T., 1973. Plant responses to water stress. Ann. Rev. Plant Physiol. 24, 519–570.
Iniesta, F., Testi, L., Orgaz, F., Villalobos, F.J., 2009. The effects of regulated and continuous deficit irrigation on the water use, growth and yield of olive trees. Eur. J. Agron. 30, 258–265.
Jones, H.G., 1992. Plants and Microclimate: A Quantitative Approach to Environmental Plant Physiology. Cambridge University Press, Cambridge.
Jones, H.G., 2004. Irrigation scheduling: advantages and pitfalls of plant-based methods. J. Exp. Bot. 55, 2427–2436.
Jones, H.G., 2007. Monitoring plant and soil water status: established and novel methods revisited and their relevance to studies of drought tolerance. J. Exp. Bot. 58, 119–130.
Marek, T., Piccinni, G., Schneider, A., Howell, T., Jett, M., Dusek, D., 2006. Weighing lysimeters for the determination of crop water requirements and crop coefficients. Appl. Eng. Agric. 22, 851–856.
Maxwell, K., Johnson, G.N., 2000. Chlorophyll fluorescence–a practical guide. J. Exp. Bot. 51, 659–668.
Moriana, A., Fereres, E., 2002. Plant indicators for scheduling irrigation of young olive trees. Irr. Sci. 21, 83–90.
Naor, A., 2006. Irrigation scheduling and evaluation of tree water status in deciduous orchards. Hort. Rev. 32, 111–166.
Pérez-López, D., Gijón, M.C., Moriana, A., 2008. Influence of irrigation rate on the rehydration of olive tree plantlets. Agr. Water Manage. 95, 1161–1166.
Ramos, A.F., Santos, F.L., 2009. Water use, transpiration, and crop coefficients for olives (cv. Cordovil), grown in orchards in Southern Portugal. Biosyst. Eng. 102, 321–333.
Sepulcre-Cantó, G., Zarco-Tejada, P.J., Jiménez-Muñoz, J.C., Sobrino, J.A., de Miguel, E., Villalobos, F.J., 2006. Detection of water stress in an olive orchard with thermal remote sensing imagery. Agric. Forest Meteorol. 136, 31–44.
Shackel, K.A., Ahmadi, H., Biasis, W., Buchner, R., Goldhamer, D., Gurusinghe, S., Hasey, J., Kester, D., Krueger, B., Lampininen, B., McGourty, G., Micke, W., Mitcham, E., Olson, B., Pelletrua, K., Philips, H., Ramos, D., Schwankl, L., Sibbett, S., Snyder, R., Southwick, S., Stevenson, M., Thorpe, M., Weinbaum, S., Yeager, J., 1997. Plant water status as an index of irrigation need in deciduous fruit trees. HortTechnology 7, 23–29.
Sofo, A., Manfreda, S., Fiorentino, M., Dichio, B., Xiloyannis, C., 2008. The olive tree: a paradigm for drought tolerance in Mediterranean climates. Hydrol. Earth Syst. Sci. 12, 293–301.
Tognetti, R., d'Andria, R., Morelli, G., Alvino, A., 2005. The effect of deficit irrigation on seasonal variations of plant water use in *Olea europaea* L. Plant Soil 273, 139–155.
Tognetti, R., d'Andria, R., Acchi, R., Lavini, A., Morelli, G., Alvino, A., 2007. Deficit irrigation affects seasonal changes in leaf physiology and oil quality of *Olea europaea* (cultivars Frantoio and Leccino). Ann. Appl. Biol. 150, 169–186.
Tripler, E., Ben-Gal, A., Shani, U., 2007. Consequence of salinity and excess boron on growth, evapotranspiration and ion uptake in date palm (*Phoenix dactylifera* L., cv. Medjool). Plant Soil 297, 147–155.
Van Bavel, C.H.M., 1961. Lysimeter measurements of evapotranspiration rates in the eastern United States. Soil Sci. Soc. Am. Pro. 25, 138–141.
Westhoff, M., Reuss, R., Zimmermann, D., Netzer, Y., Gessner, A., Geßner, P., Zimmermann, G., Wegner, L.H., Bamberg, E., Schwartz, A., Zimmermann, U., 2009. A non-invasive probe for online-monitoring of turgor pressure changes under field conditions. Plant Biol. 11, 701–712.
Zimmermann, D., Reuss, R., Westhoff, M., Geßner, P., Bauer, W., Bamberg, E., Bentrup, F.-W., Zimmermann, U., 2008. A novel, non-invasive, online-monitoring, versatile and easy plant-based probe for measuring leaf water status. J. Exp. Bot. 59, 3157–3167.